Cilt 9, Sayı 2, Sayfa 1-8, 2020 Volume 9, Issue 2, Page 1-8, 2020

Araştırma Makalesi https://doi.org/10.46810/tdfd.822928 Research Article

Türk Doğa ve Fen Dergisi
Turkish Journal of Nature and Science
www.dergipark.gov.tr/tdfd

Synthesis and Characterization of Pollen Extract Mediated Gold Nanostructures

Fatma BAKAR[1,2], Hamide Ayçin SÖNMEZ[2], Senanur EVECEN[2], Buse TURAN[1], Mehmet Ali DEMİR[1], Abdurrahman GÜMÜŞ[3], Talip ÇETER[4], İdris YAZGAN[1*]

[1] Center of Materials and Biosensors, Department of Biology-Kastamonu University, Turkey
[2] Kastamonu Science and Art Center, Turkey
[3] Department of Electrical and Electronics Engineering, İzmir İstitute of Technology, İzmir Turkey
[4] Center for Aerobiology, Department of Biology-Kastamonu University, Turkey
Fatma BAKAR ORCID No: 0000-0002-3999-0983
Hamide Ayçin Sönmez ORCID No: 0000-0002-2580-9792
Senanur Evecen ORCID No: 0000-0001-6325-2123
Buse Turan ORCID No: 0000-0003-4196-8969
Mehmet Ali Demir ORCID No: 0000-0001-7726-431X
Abdurrahman Gümüş ORCID No: 0000-0003-2993-5769
Talip Çeter ORCID No: 0000-0003-3626-1758
İdris YAZGAN ORCID No: 0000-0002-0264-1253

**Corresponding author: iyazgan@kastamonu.edu.tr*

(Alınış: 07.11.2020, Kabul: 30.11.2020, Online Yayınlanma: 30.12.2020)

Keywords
Gold nanostructure, Gold nanorod, Pollen grain extract, Green synthesis

Abstract: There is an increasing demand in the synthesis of shape and size-controlled gold nanostructures (Au NSs) with greener methods. Therefore, we aimed to synthesize differently shaped and sized Au NSs using a greener technique under ambient conditions. In this study, we utilized pollen extracts of Corylus avellana, Juniperus oxycedrus and Pinus nigra species (collected from Kastamonu region of Turkey) for the synthesis. The extraction was performed in water in order to recover "water soluble" content from the pollen grains. The extracts were used to stabilize, and direct shape and size of the HEPES (4-(2-hydroxyethyl)-1-piperazineethanesulfonic acid) buffer synthesized Au NSs. UV-vis, powder X-ray diffraction (PXRD), scanning electron microscopy (SEM) characterizations proved synthesis of spherical, anisotropic and large Au NSs with this benign approach. The obtained Au NSs were possible to separate small and large Au NSs through centrifugation. Chemistry of pollen extracts played a key role on the morphology and stability of the Au NSs. The findings, for the first time, is revealing the synthesis of large Au nanorod bundles (>300 nm) along with hexagonal and spherical Au NSs under ambient conditions using pollen grain extracts, whose maturation took 24h.

Polen Özütü Aracılı Altın Nanoparçacıkların Sentezi ve Karakterizasyonu

Anahtar Kelimeler
Altın nanoyapı, Altın nanorod, Pollen tane özütü, Yeşil kimya sentezi

Öz: Altın nanoyapıların (AuNYların) morfoloji ve boyut kontrollü sentezlerinin yeşil kimya ile sentezine ihtiyaç giderek artmaktadır. O nedenle biz bu çalışma da AuNYlarının boyut ve morfoloji kontrollerinin oda şartlarında sentezini çalıştık. Kastamonu bölgesinden toplanan Corylus avellana, Juniperus oxycedrus ve Pinus nigra türlerine ait polen özütlerini kullanarak sentezler gerçekleştirildi. Polen tanelerinden özütleme saf su içerisinde gerçekleştirilerek su da çözünen bileşenlerin izolasyonu hedeflendi. Özütler, HEPES (4-(2-hidroksimetil)-1-piperazinetan sülfonik asit) tamponu aracılığıyla sentezlenmiş AuNYların kararlılığı ve şekil/boyut yönlendirilmesinde rol oynamıştır. UV-Vis, toz X-ışınları krınım tekniği ve taramalı elektron mikroskobu çalışmaları sentezlenen AuNYların sferik, anizotropik ve büyük yapı morfolojilerine sahip olduğunu göstermiştir. AuNYlar santrifüj kullanılarak boyutlarına göre ayrılmışlardır. Polen kimyasının sentezlenen AuNYların kararlılığı ve morfolojilerinde anahtar rol oynadıklarını göstermiştir. Araştırmalarımıza göre bu çalışma ile hekzagonal ve sferik AuNYlara ek olarak >300 nm nanorod demetlerin polen tane ekstraksiyonları ile oda sıcaklığında sentezi ilk defa gerçekleştirilmiştir. Sentezlenen AuNYların morfolojik kararlılıkları 24 saat içerisinde tamamlanmıştır.

1. INTRODUCTION

Green synthesis of metallic nanomaterials are of great interests owing to their sustainable production and being free from environmentally toxic chemicals [1]. Utilization of plant extracts [2–5], simple sugars [6], microorganisms [7] and carbohydrate polymers [6] are among the greener approaches. Among these approaches, the use of plant extracts are the most widely preferred route in the synthesis of metallic nanostructures including gold [6], silver [8], copper [9] and platinum [10]. Similarly, pollen grains have been shown as a reactor in metallic nanomaterials synthesis [11] as well as that their extracts provide proper chemistry in the synthesis of shape and size directed metallic nanostructures [12,13].

There is an increasing demand in synthesis of shape and size controlled Au NSs along with surface chemistry control in accordance with the application requirements [14]. Pollen grains contain carbohydrates, proteins, amino acids and phenolic compounds [15]. Extraction methods can allow targeted isolation of chemical constituents from pollen grains [16]. Even though pollen grains are of seasonal allergens [17,18], they have been exploited for biotechnological applications [19]. Despite the fact that pollen extracts are rich of bioactive molecules that can provide stabilization and capping for metallic nanostructures during their wet-chemistry mediated synthesis [13], their utilization has been rather limited. Limited studied regarding on polen extracted nanostructure materials have been found in the literature.

In this study, we utilized extracts of pollen grains from Corylus avellana, Juniperus oxycedrus and Pinus nigra species collected in Kastamonu province of west black-sea region of Turkey. “Water soluble” organic constituents and biomolecules (e.g. protein and sugars) have differences among these species pollen grains based on the obtained IR data. Water-based extraction applied to the pollen grains to collect “water soluble” molecules to prevent extra steps so as to solubilize the synthesized nanostructures. It is known that aqueous extraction of pollen grains, independent from the pollen species, reveal release of amino acids [20], carbohydrates and proteins [15]. HEPES buffer was used to initiate Au NSs formation while the extracts served as the directing, capping and stabilizing agents. The type of pollen extracts with its addition method brought dramatic effects on the Au NSs size and morphology.

2. MATERIALS AND METHODS

N-(2-Hydroxyethyl)piperazine-N′-(2-ethanesulfonic acid) (HEPES, ≥ 99.5%) and gold (III) chloride trihydrate (HAuCl4·3H2O, 99.995 %), DPPH (2,2-diphenyl-1-picrylhydrazyl, ≥ 97 %) reagent, absolute ethanol (≥ 99.8%) were purchased from Sigma-Aldrich. De-ionized (DI) water with resistivity of 18.2 MΩ was produced by Humana Zeneer power 1 used throughout the study.

2.1 Extraction of Active Ingredients from Pollens

The plants belong to different families as Corylus avellane (CA) is a member of Betulacea, Juniperus oxycedrus (JO) is member of Cupressaceae family [21] while Pinus nigra (PN) is a member of Pinaceae family [22], whose pollen grains were used in the study that were collected in 2017 in Kastamonu. 1 g of pollen from each species were added into 10 mL DI water, which was kept at 60 °C for 4 h. Every 30-min, the mixture was gently vortexed to enhance release of the water-soluble active ingredients. The mixture was then centrifuged at 5000 rpm for 10 min to precipitate pollen debris. Supernatant part was finally filtered through a 0.22 µm sterile filter. The extract was frozen at -82 °C, followed by lyophilization in Christ Alpha 1-2 LD Freeze Dryer lyophilizer. ATR-FTIR (Bruker, Alpha II) in the region between 4000-400 cm-1 was used to characterize the functional groups of the extracts.

2.2 Antioxidant Capacity of the Pollen Extracts

DPPH (2,2-diphenyl-1-picrylhydrazyl) assay was used to characterize antioxidant potential of the pollen extracts using 0.16 M DPPH prepared in absolute ethanol. All pollen extracts were used at 0.75 mg/mL concentration, and incubation time was kept as 5-min.

2.3 Au NS Synthesis

Ratio of pollen extracts and HEPES buffer (pH 7.4) were optimized to obtain colloidally stable nanostructures. Concentration of HEPES buffer was tested between 100 mM and 10 mM while pollen concentration varied between 5 mg/mL to 0.75 mg/mL. HAuCl4·H2O concentrations were tested at 0.5 mg/mL to 0.15 mg/mL. **Table 1** summarizes the synthesis conditions for Au nanostructures.

Table 1: Pollen extracts mediated synthesis of Au nanostructures using HEPES as reducing agent.

Sample Name	HEPES[1] (µL)	DI water (µL)	*Pollen extract*[2] (µL)	$HAuCl_4 \cdot H_2O$[3] (µL)
Approach 1 Pollen extracts introduced to the media with HEPES before $HAuCl_4 \cdot 3H_2O$ introduction				
HP1	1000	960	0	40
HP2	1000	940	0	60
PN1	1000	700	260	40
PN2	1000	700	240	60
JO1	1000	700	260	40
JO2	1000	700	240	60
CA1	1000	700	260	40
CA2	1000	700	240	60
***Approach 2**: Pollen extract introduced to the media 1-min after mixing HEPES and* $HAuCl_4 \cdot 3H_2O$				
PN3	1000	700	260	40
JO3	1000	700	260	40
CA3	1000	700	260	40
PN4	1000	700	240	60

2.5 Characterization of Au NSs

UV-Vis spectrometry (T60 PG Instrument), powder X-Ray diffraction (Philips X'Pert Pro), Scanning Electron Microscopy (SEM) (FEI QUANTA 250 FEG) were used to characterize surface plasmon resonance, crystal structure and morphology, respectively. 400-mesh (01896N) Ted-Pella grids were used for SEM analysis.

3. RESULTS AND DISCUSSIONS

3.1 Antioxidant Potential and Functionality of the Pollen Extracts

Due to the fact that the goal of the study was to synthesize gold nanostructure with a fast kinetic in aqueous system under ambient conditions, DPPH reduction by the pollen extracts was confined to 5-min. A common approach (Equation 1) to reveal extracts radical scavenging capability is to calculate relative DPPH reduction was followed in the study.

$$\%\ Reduction = [\frac{(Abi-Abs)}{Abi}]X100 \qquad \text{Equation 1:}$$

where Ab_i refers to the absorbance of DPPH concentration while Abs refers to the absorbance for the sample after 5-min incubation [23]. % DPPH reduction for the pollen extracts were found as 80.7, 38.6 and 80.5 for CA, JO and PN respectively.

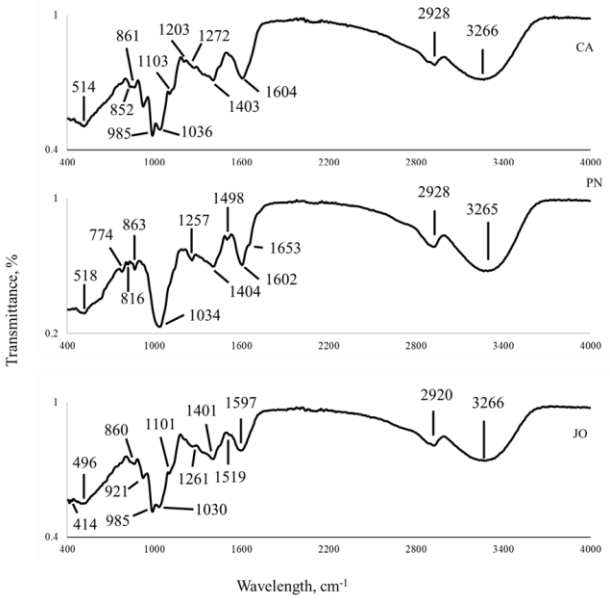

Figure 1: IR spectra of aqueous extracts of CA, PN and JO pollen grains.

It is clear that CA and PN possessed the same DPPH reduction capacity while JO gave less than half of DPPH in comparison to CA and PN. Differences in antioxidant capacity of the pollen extracts can be related to the presence of different antioxidant compounds that pollen grains have. It is possible that high antioxidant activity of CA and PN can be resulted from high load of conjugated [15] and polyphenols [24]. For instance, CA pollen grains contain high load of carotenoids [15]. Besides, water mediated extraction can trigger release of proteins, sugars, amino acids, carotenoids, glycosylated flavonoids and free amino acids [15]. As detained below, CA extract has carotenoids, conjugated constituents that give CA extract high radical scavenging activity. Similarly, PN and JO extracts gave conjugated structures (e.g. flavonoids). The differences between the antioxidant activities are possibly related to type of flavonoids and their amounts along with such other structures including carotenoids and the side groups in proteins.

FTIR studies revealed (**Figure 1**) that CA, PN and JO pollen grain aqueous extracts have proteins (~1600 cm-1 for C=O stretching of amide group, and C–O, C–N and C–C stretching vibrations for ~1030 cm-1) [25,26] and saccharides (920-700 cm-1 for vibration of C–OH groups and ~1030 cm-1 stretching vibration for C-C group) [25]. It is important to mention that the peak at ~1600 cm-1 can also represent the presence of carotenoids [15]. Among the extracts, only CA gave bright yellow color, so the peak for CA is more from carotenoid, but the same thing cannot be said for JO and PN extracts. Interestingly, all the spectra revealed the presence of RNA with the band at ~860 cm-1 of C-O-P-O-C [15]. Flavonoid peaks locate between 669-411 cm-1 [27]; 514 cm-1 of CA extract, 518 cm-1 of PN and 496 and 414 cm-1 of JO were obtained. Even though, clear peaks were not observed for phenolic acids, shoulders between 1800-1500 cm-1 reveals presence of phenolic acids [25] for all the extracts.

Particularly, the bands at 1519 cm-1 of JO and at 1653 cm-1 of PN (more of a shoulder peak) represent presence of proteins [28], which means that JO and PN extracts have more protein content than CA extract. Besides, the band at 1653 cm-1 of PN represents presence of α-helical proteins [28], which is not present in the other extracts. In contrast to this, any band at ~ 720 for cm-1 (characteristic peak for CH2 rocking of lipids) was not observed for any of the extracts. So, it is possible to speculate that the peak at ~2928 cm-1 is the sign for presence of cellulose instead of lipids. It is noteworthy to mention that band intensities for the same group is proportional to the concentration of the functional group [26]. Particularly at ~1030 cm-1 PN gave stronger band, which could refer to that PN extracts exhibiting, or possessing, a higher amount of saccharides in comparison to CA and JO extracts.

Comparison of the fingerprint region (1800-500 cm-1) for all the extracts gave different signatures: for instance, PN spectrum gave clear band at 774 cm-1, which is seen as a shoulder in the JO spectrum. Similarly, PN spectrum gave characteristic α-glycosidic bond at 816 cm-1 while the band at 1257 cm-1 refers to in-plane bending vibration of -OH group [29]. CA spectrum gave characteristic absorption at 1203 cm-1 ascribed to phosphate groups (nucleic acids and phospholipids) [30] while CA and JO gave strong absorption at 985 cm-1 due to the presence of carbohydrates (from C-O or C-C bonds) [31]. In contrast to this, all the extracts gave absorption band at ~ 860 cm-1 , typical of anomeric region of carbohydrates [31], while PN extract gave the sharpest peak. The bands at ~1100 cm-1 are due to C-O

of alcohol group in CA and JO. The band at 852 cm-1 of CA extract refers to the presence of aromatic groups [32] of sporopollenin.

3.2 Synthesis and Characterization of Au Nanostructures

HEPES buffer, inherently a week reducing agent, is among the buffers widely utilized in synthesis of metallic nanostructures. Even though it can reduce Au3+ ions to metallic Au, during formation of stabilized Au NSs, its molar ratio to Au3+ ions poses critical importance as much as its pH [33]. In our study, we tested HEPES buffer at pH 6.0 and 7.4 (25 mM in both cases) to initiate Au NSs nucleation. As given in **Table 1**, we selected 25 mM pH 7.4, which improved nanostructure synthesis kinetics as well as that the pH was kept near to neutral. During the study, HEPES triggered Au NSs synthesis within 5-minutes.

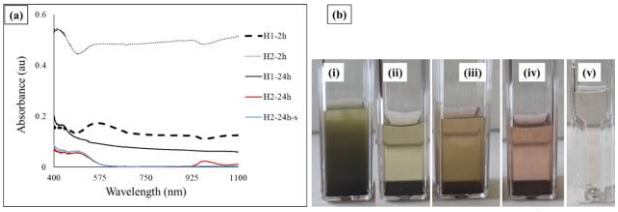

Figure 2: UV-Vis spectra (a) and digital micrographs (b) of HEPES synthesized Au NSs. (i) H1-2h, (ii) H1-24h, (iii) H2-2h, (iv) H2-24h and (v) H2-24-s, where s refers to the supernatant after centrifugation at 5000 rpm for 15 min.

As illustrated in **Figure 2**, at higher HEPES/Au3+ ratio a clear two SPR peaks at around 570 nm and 890 nm were obtained (H1-2h) with a green color, which started precipitating within 2 h (**Figure 2b-i**). As shown in **Figure 2b-ii**, all NSs precipitated within 24 h, where the supernatant did not give any SPR peak (H1-24h) around characteristic Au nanostructure range wavelengths (> 500 nm). In contrast to this, at lower HEPES/Au3+ ratio a wide SPR peak from 560-900 nm was obtained that refers to NSs over 200 nm [34]. Even though at lower ratio, precipitation was maximum within 2 h (**Figure 2b-ii**), its supernatant (**Figure 2b-iv**) gave 2 SPR peaks at ~ 503 nm (more of spherical with < 10 nm size) and at 980 nm (highly anisotropic Au NSs) (H2-24h). Centrifugation resulted in loss of the peak at 980 nm (H2-24h-s) along with decreased intensity of the supernatant's color (**Figure 2b-v**). Therefore, it can be said that at proper HEPES/Au3+ ratio (at pH 7.4 with 25 mM/4.41 mM) stable colloidal Au NSs can be obtained under the tested conditions. Anisotropic Au NSs in precipitates are shown in **Figure 3**.

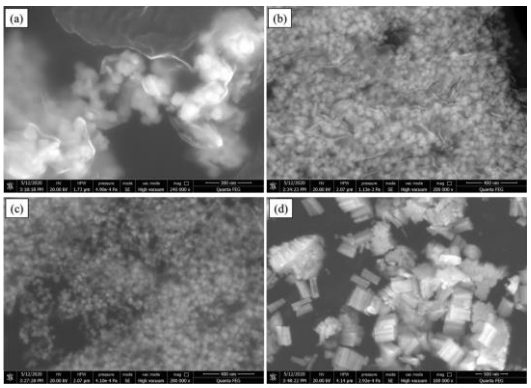

Figure 3: SEM micrographs of precipitated Au NSs for (a) HP2-24h-s, (b) PN2-24h-s, (c) JO2-24h-s and (d) PN4-24h-s.

Pollen grain extracts were applied to stabilize HEPES synthesized Au NSs in two ways as the extracts were mixed with HEPES buffer, followed by HAuCl4·H2O solution addition. In the second approach, pollen extracts were added to HEPES-HAuCl4·H2O mixture 1 min later. Both approaches allowed synthesis of stable spherical and anisotropic Au NSs (**Figure-3** and **-4**). The extracts at 1.95 mg/mL and 1.8 mg/mL concentrations were used for 2.94 mM and 4.41 mM Au3+ ion concentration, respectively.

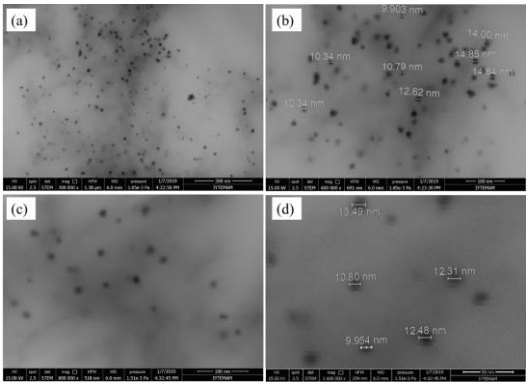

Figure 4: SEM micrographs of JO1-24h-s (a and b) and PN4-24h-s (c and d).

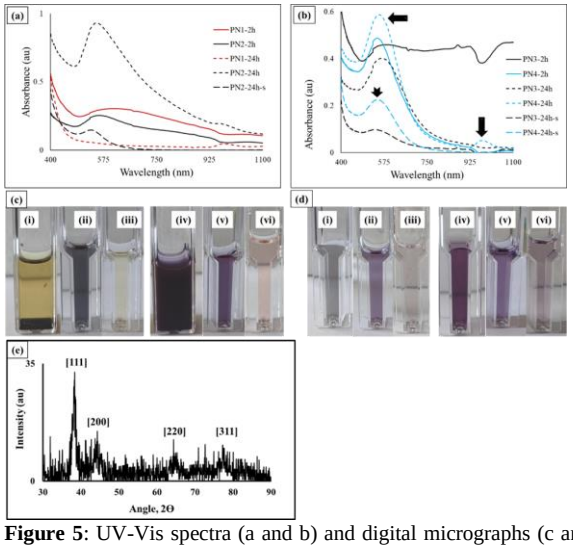

Figure 5: UV-Vis spectra (a and b) and digital micrographs (c and d) of *PN* extract stabilized Au NSs. In c, (i) PN1-2h, (ii) shaken and diluted PN1-2h, (iii) diluted PN1-24h, (iv) PN2-2h, (v) diluted PN2-24h and (vi) PN2-24h-s. In (d), (i) diluted PN3-2h, (ii) diluted PN3-24h, (iii) PN3-24h-s (iv) diluted PN4-2h, (v) diluted PN4-24h, and (vi) PN4-24h-s (s refers to the supernatant after centrifugation at 5000 rpm for 15 min). e) XRD pattern of PN4 indexed to *fcc* Au crystal structure (ICDD PDF no: 000-004-0784).

Introduction of pollen grain extracts posed dramatic effect on Au NSs formation and stability. **Figure 5a** reveals that PN1-2h have a wide SPR spectrum between 500-950 nm (Au NSs > 200 nm) that gave greenish color when the precipitate was shaken (**Figure 5c-ii**), which got lost upon 24 h incubation (PN1-24h). PN1 precipitated within 2h (**Figure 5c-i**) and gave a clear solution within 24 h (**Figure 5c-iii**). At higher PN extract/Au3+ ratio (PN2-2h and PN2-24h), stable Au NSs were obtained (**Figure 5c-iv** and **-v**). Even though PN2 protected its stability, centrifugation changed its color from purple (**Figure 5c-v**) to light pink (**Figure 5c-iii**). SPR peaks at 555 nm and 967 nm (PN2-24h) disappeared and only SPR peak at 540 nm (PN2-24h-s) remained through centrifugation (notched arrow in **Figure 5b**). This is attributed to enhanced gravity related precipitation of larger NSs (see **Figure 4**).

Figure 5b shows that PN3-2h gave a broad SPR spectrum from 520-950 nm, which then turned into a sharp single peak at 570 nm. Based on the literature, this observation can be related to that single NS gathered to form larger assemblies (greenish color, **Figure 5d-i**), followed by detachment to single Au NSs through adsorption/reaction of PN extracts on the formed Au NSs (purple color, **Figure 5d-ii**). Centrifugation, as expected, resulted in blue shifts (from 570 nm to 540 nm), whose color turned into pale pink (**Figure 5d-iii**). Interestingly, lower PN extract/Au3+ ion ratio gave faster maturation for Au NSs synthesis as seen in **Figure 5** (PN4-2h and PN4-24h) and in **Figure 5d** (**Figure 5d-iv and -v**). Similar to PN3, centrifugation altered the color of the supernatant (**Figure 5d-vi**). However, it should be noted that PN4-24 gave extra peak at 977 nm, representing nanorod formation (**Figure 3-d**). SPR peaks at NIR region can allow nanostructure to be considered for biomedical analyses [35], which type of NSs can be obtained using the pollen extracts, followed by benchtop centrifuge. Formation of nanorod bundle is probably related to presence of both α-helices and β-sheet protein content of PN extracts since proteins can serve as temple in gold nanorod synthesis [36].

It is known that HEPES mediated Au NSs give fcc crystal structure [22], so as an illustration crystal structure of pollen directed Au NSs synthesized in HEPES, PN4 was selected to exemplify the crystal structure of the synthesized Au NSs as shown in **Figure 5e**. Miller indices of (111), (200), (220) and (311) is the representation of fcc crystal structure (ICDD PDF: 000-004-0784; International Centre for Diffraction Data) [23].

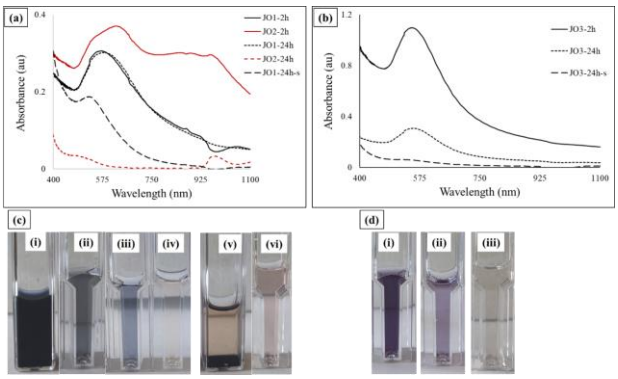

Figure 6: UV-Vis absorption spectra (a and b) and digital micrographs (c and d) of *JO* extract stabilized HEPES synthesized Au NSs. In c, (i) JO1-2h, (ii) diluted JO1-2h, (iii) diluted JO1-24h, (iv) JO1-24h-s (v) JO2-2h, and (vi) JO2-24h-s. In (d), (i) diluted JO3-2h, (ii) diluted JO3-24h, (iii) JO3-24h-s, where s refers to the supernatant after centrifugation at 5000 rpm for 15 min.

JO pollen grain extracts triggered maturation within two hours incubation (JO1-2h and JO1-24h) with a sharp SPR peak at 580 nm, whose centrifugation triggered blue shift (SPR peak shifted to 532 nm). No precipitation occurred within 24 h (**Figure 6c-i** and **-iii**) while centrifugation altered the color from blueish to pale pink (**Figure 6c-iv**). In contrast to this, at lower ratio (JO2) fully precipitated (**Figure 6c-v**), whose shaken version gave greenish color (**Figure 6c-vi**) with an SPR spectrum resembling formation of dimer/trimer from single Au NSs [34]. Maturation of JO2 (JO2-24h) gave two SPR peaks at 502 nm and 975 nm, which refer to anisotropic Au NSs formation, whose centrifugation resulted in colorless supernatant with no SPR peak (data not shown). As shown in **Figure 6b**, addition of the extract after mixing HEPES and HAuCl4·H2O solutions gave stable purple colored solution (**Figure 6d-i and -ii**) with SPR peaks at ~ 562 nm, whose centrifugation caused blue shift to 532 nm (JO3-24h-s) with very pale pink color (**Figure 6d-iii**).

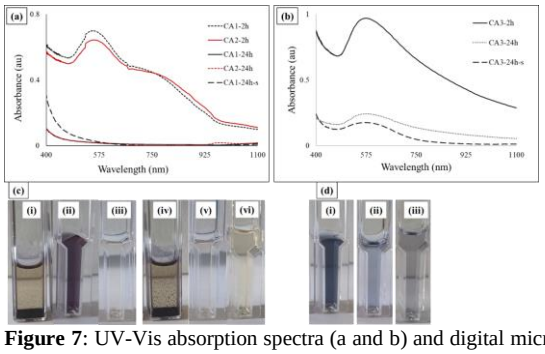

Figure 7: UV-Vis absorption spectra (a and b) and digital micrographs (c and d) of CA extract stabilized HEPES synthesized nanostructured. In c, (i) CA1-2h, (ii) shaken and diluted CA1-2h, (iii) CA1-24h, (iv) CA2-2h, (v) CA2-24h and (vi) CA2-24h-s. In (d), (i) diluted CA3-2h, (ii) diluted CA3-24h, (iii) CA3-24h-s, where s refers to the supernatant after centrifugation at 5000 rpm for 15 min.

CA pollen grain extracts for both tested concentrations according to Approach 1 did not give stable Au NSs. Both CA1 and CA2 precipitated (**Figure 7c-i** and **-iv**) within 2 h, whose shaken mixture (**Figure 7c-ii**) gave two SPR peaks (CA1-2h and CA2-2h). Incubation up to 24 h resulted in clear supernatant (**Figure 7c-iii** and **-v**) and further centrifugation gave similar color (**Figure 7c-vi**). The supernatants at 24 h incubation (CA1-24h, CA2-

24h and CA2-24h-s) did not give any SPR peaks belonging to AuNSs. In contrast to these, CA pollen grain extracts triggered stable Au NSs formation in Approach 2. Two hours incubation (CA3-2h) gave SPR peak at 574 nm with strong bluish color while ripening gave red shift to 584 nm (CA3-24h), whose centrifugation reversed the SPR peak back to 547 nm (CA3-24h-s). Even though the intensity of the color changed during centrifugation to pale blue (**Figure 7d-iii**), the difference between **Figure 7c-i** and **-ii** is only related to the amount of aliquot placed into the cuvette for UV-Vis analysis. However, stability of CA mediated AuNSs were not high (completely clumped within 48 h and require extensive vortexing) so further morphological analysis were not performed. This could be related to that CA extract gave lesser amount of proteins and carbohydrates than PN and JO extract, where proteins and carbohydrates can serve as stabilizing agent [36,37].

In all cases 24 h was enough to complete Au NSs synthesis at room temperature. 48 h and 72 h incubation did not alter SPR peaks of any of the Au NSs in supernatants (data not shown). Au NSs in the precipitates are not expected to alter their morphology since they are isolated from the ligands found in the extracts. The pollen grain extracts were tested alone in the synthesis of Au NSs, but none of them initiated particle nucleation within 2 hours, that is why they were not tested alone. There was no correlation between antioxidant capacity and Au NSs formation/stability for the tested pollen grain extracts. In contrast to this, even though CA showed similar antioxidant capacity to PN extract, stable Au NSs were not obtained. However, chemical character of the pollen grain extracts posed dramatic effect on the Au NSs morphology and stability.

Since Au NSs synthesized using JO and PN extracts gave very characteristic SPR spectra and stable Au NSs, SEM and STEM based morphology analyses were performed for them. As seen from **Figure 4**, centrifugation mediated precipitation provided separation for large and smaller AuNSs. JO1-24h-s (**Figure 3**) gave spherical Au NSs with 11±2 nm size range while the precipitated of JO2-24h-s (Figure 4) gave 25±5 (~ 50 %) and 35±5 (~ 50 %) sized anisotropic Au NSs. Similarly, PN2-24h-s (**Figure 3**) gave ~ 12±2 nm sized spherical Au NSs, whose precipitate gave anisotropic Au NSs with sizes of 45±3 x 55±7 nm hexagonal and 25±3 x 32±3 nm hexagonal morphology (**Figure 4**). Besides, minor amount (<10 %) of spherical Au NSs with 15±5 nm diameter. Interestingly, precipitate of PN4-24-s gave rod shaped Au NSs with an average length of 302 ±5 nm and width of 55 ±10 nm (**Figure 4**), which gave two SPR peaks characteristics for nanorods (depicted with arrows in **Figure 5b**). This shows that introduction of pollen extract into HEPES/HAuCl4 mixture before reaction and/or after reaction can bring dramatic effect on the NS morphology and size. In the case of HEPES-mediated Au NSs synthesis (**Figure 4**), overwhelmingly tetragonal and hexagonal morphology with 70 x 80 ±5 nm, 80 x 80 ±5 nm size range and minor amount of rod-shaped with 143 x 35 nm sized Au NSs were obtained. It is possible that the supernatant of HP2 might have spherical and small sized (<20 nm) nanostructure based on **Figure 3**.

Due to the fact that colloidal Au NSs with high purity and possible minimum size and shape diversity are critical for their applications, their synthesis and post-synthesis procedures have been under thorough investigations [34]. Centrifugation is a valuable approach to selectively isolate metallic nanostructures based on size and shape [38]. Centrifugation applied to the Au NSs synthesized in the presence of pollen extracts allowed separation of differently sized Au NSs with characteristic morphology. It is possible that further refinement for narrower size and shape separation with centrifugation [34], which can tune the collected Au NSs samples. Another important thing is that anisotropic NSs have critical places in catalysis, sensor support materials, optics and electronics [39,40]. Therefore, their directed synthesis and isolation are critical. Particularly, synthesis of rod shaped nanostructures possessing > 100 nm length requires extreme conditions and use of toxic chemicals like CTAB [41]. Hereby, we synthesized ordered very large Au NSs utilizing green chemistry through the use of pollen extracts.

4. CONCLUSION

Greener approaches in synthesis of metallic nanostructures are among the most widely studied routes for nanostructure studies. Hereby, we utilized water extracts of pollen grains from three different pollen species using HEPES buffer as initiator of gold (iii) ion. Type of pollen species and introduction method of pollen extract to direct shape and size growth posed dramatic effect on the synthesized AuNSs in relation to the chemical composition of the pollen extracts. Reduction capability of the pollen extract did not give any correlation for the speed of Au NSs synthesis and morphology control because of the fact that these groups provided radical scavenging activity, did not serve as stabilizing agent. 24 h was enough to have mature Au NSs under ambient conditions. Based on the results, it is possible to have fine control on morphology and size on the synthesized Au NSs by controlling the ratio of pollen extract/Au3+ ion, which can be further refined by using centrifugation at different centrifugal force. Based on our literature survey, this is the first study that reports on the synthesis of large gold nanorods using pollen extracts. Further qualitative and quantitative spectroscopic and chromatographic characterizations of the extracts are required to enlighten which functional groups play the most critical role in the size and shape directing effect on the Au NSs along with their stabilization..

Acknowledgements

Many thanks to Prof Muhammet S Toprak of KTH Royal Institute of Technology (Stockholm, Sweden) for his guidance and review of the manuscript. We also acknowledge BIOMER center of İzmir Institute of Technology and Central Research Laboratory of Kastamonu University for SEM studies. This study was supperted by Kastamonu University with the project number KÜ-BAP01/2018-33.

REFERENCES

[1] O. V. Kharissova, H.V.R. Dias, B.I. Kharisov, B.O. Pérez, V.M.J. Pérez, The greener synthesis of nanoparticles, Trends Biotechnol. 31 (2013) 240–248. https://doi.org/10.1016/j.tibtech.2013.01.003.

[2] P. Vijaya Kumar, S. Mary Jelastin Kala, K.S. Prakash, Green synthesis of gold nanoparticles using Croton Caudatus Geisel leaf extract and their biological studies, Mater. Lett. 236 (2019) 19–22. https://doi.org/10.1016/j.matlet.2018.10.025.

[3] V. V. Makarov, A.J. Love, O. V. Sinitsyna, S.S. Makarova, I. V. Yaminsky, M.E. Taliansky, N.O. Kalinina, "Green" nanotechnologies: Synthesis of metal nanoparticles using plants, Acta Naturae. 6 (2014) 35–44. https://doi.org/10.1039/c1gc15386b.

[4] M. Jamzad, M. Kamari Bidkorpeh, Green synthesis of iron oxide nanoparticles by the aqueous extract of Laurus nobilis L. leaves and evaluation of the antimicrobial activity, J. Nanostructure Chem. 10 (2020) 193–201. https://doi.org/10.1007/s40097-020-00341-1.

[5] A.A. Jenifer, B. Malaikozhundan, S. Vijayakumar, M. Anjugam, A. Iswarya, B. Vaseeharan, Green Synthesis and Characterization of Silver Nanoparticles (AgNPs) Using Leaf Extract of Solanum nigrum and Assessment of Toxicity in Vertebrate and Invertebrate Aquatic Animals, J. Clust. Sci. 31 (2020) 989–1002. https://doi.org/10.1007/s10876-019-01704-7.

[6] C. Engelbrekt, K.H. Sørensen, J. Zhang, A.C. Welinder, P.S. Jensen, J. Ulstrup, Green synthesis of gold nanoparticles with starch–glucose and application in bioelectrochemistry, J. Mater. Chem. 19 (2009) 7839. https://doi.org/10.1039/b911111e.

[7] N.N. Dhanasekar, G.R. Rahul, K.B. Narayanan, G. Raman, N. Sakthivel, Green chemistry approach for the synthesis of gold nanoparticles using the fungus Alternaria sp, J. Microbiol. Biotechnol. 25 (2015) 1129–1135. https://doi.org/10.4014/jmb.1410.10036.

[8] M. Jha, N.G. Shimpi, Green synthesis of zero valent colloidal nanosilver targeting A549 lung cancer cell : In vitro cytotoxicity, J. Genet. Eng. Biotechnol. 16 (2018) 115–124. https://doi.org/10.1016/j.jgeb.2017.12.001.

[9] I. Chung, A.A. Rahuman, S. Marimuthu, A.V. Kirthi, K. Anbarasan, P. Padmini, G. Rajakumar, Green synthesis of copper nanoparticles using eclipta prostrata leaves extract and their antioxidant and cytotoxic activities, Exp. Ther. Med. 14 (2017) 18–24. https://doi.org/10.3892/etm.2017.4466.

[10] J.Y. Song, E.Y. Kwon, B.S. Kim, Biological synthesis of platinum nanoparticles using Diopyros kaki leaf extract, Bioprocess Biosyst. Eng. 33 (2010) 159–164. https://doi.org/10.1007/s00449-009-0373-2.

[11] Y. Xiaohui, S. Xiuqin, W. Yu, W. Wei, S. Yuhan, H. Lixue, Preparation of Spinous ZrO2 Microspheres with Tunable Shell and Chamber Structure by Controlling Pollen as a Nanoparticles Reactor, J. Nanosci. Nanotechnol. 11 (2011) 10369–10373. https://doi.org/10.1166/jnn.2011.5020.

[12] S. Hajebi, M. Homayouni, T. Mahboobeh, N. Moghaddam, F. Shahraki, Rapeseed flower pollen bio - green synthesized silver nanoparticles : a promising antioxidant , anticancer and antiangiogenic compound, JBIC J. Biol. Inorg. Chem. 24 (2019) 395–404. https://doi.org/10.1007/s00775-019-01655-4.

[13] H. Banu, N. Renuka, S.M. Faheem, R. Ismail, V. Singh, Z. Saadatmand, S.S. Khan, K. Narayanan, A. Raheem, K. Premkumar, G. Vasanthakumar, Gold and Silver Nanoparticles Biomimetically Synthesized Using Date Palm Pollen Extract-Induce Apoptosis and Regulate p53 and Bcl-2 Expression in Human Breast Adenocarcinoma Cells, Biol. Trace Elem. Res. 186 (2018) 122–134. https://doi.org/10.1007/s12011-018-1287-0.

[14] J.P. Sylvestre, S. Poulin, A. V. Kabashin, E. Sacher, M. Meunier, J.H.T. Luong, Surface chemistry of gold nanoparticles produced by laser ablation in aqueous media, J. Phys. Chem. B. 108 (2004) 16864–16869. https://doi.org/10.1021/jp047134.

[15] B.G. Pummer, H. Bauer, J. Bernardi, B. Chazallon, S. Facq, B. Lendl, K. Whitmore, H. Grothe, Chemistry and morphology of dried-up pollen suspension residues, J. Raman Spectrosc. 44 (2013) 1654–1658. https://doi.org/10.1002/jrs.4395.

[16] Z.F. Feng, X.F. Chen, D.L. Di, Online extraction and isolation of highly polar chemical constituents from Brassica napus L. pollen by high shear technique coupled with high-performance counter-current chromatography, J. Sep. Sci. 35 (2012) 625–632. https://doi.org/10.1002/jssc.201100992.

[17] N.M. Pinar, K. Gu, A. Yildiz, M. Smith, A 2-year aeropalynological survey of allergenic pollen in the atmosphere of Kastamonu , Turkey, Aerobiologia (Bologna). 28 (2012) 355–366. https://doi.org/10.1007/s10453-011-9240-0.

[18] Y. Türkmen, T. Çeter, N.M. Pinar, Analysis of airborne pollen of Gümüşhane province in northeastern Turkey and its relationship with meteorological parameters, Turk. J. Botany. 42 (2018) 687–700. https://doi.org/10.3906/bot-1712-39.

[19] M. Mujtaba, M. Kaya, T. Ceter, An investigation of pollen grain thermal diversity on species level, Commun. Fac. Sci. Univ. Ankara Ser. C Biol. 27 (2018) 170–176. https://doi.org/10.1501/commuc.

[20] S. Seifert, V. Merk, J. Kneipp, Identification of aqueous pollen extracts using surface enhanced Raman scattering (SERS) and pattern recognition methods, J. Biophotonics. 9 (2016) 181–189. https://doi.org/10.1002/jbio.201500176.

[21] A. Acar, N.M. Pınar, F. Şafak, S. Silici, Analysis of Airborne Pollen Grains in Kayseri , Turkey, Karaelmas Fen ve Mühendislik Derg. 5 (2015) 79–88.

[22] B. Zimmermann, A. Kohler, Infrared spectroscopy of pollen identifies plant species and genus as well as environmental conditions, PLoS One. 9 (2014). https://doi.org/10.1371/journal.pone.0095417.

[23] J. Deng, W. Cheng, G. Yang, A novel antioxidant activity index (AAU) for natural products using the DPPH assay, Food Chem. 125 (2011) 1430–1435. https://doi.org/10.1016/j.foodchem.2010.10.031.

[24] T. Hofmann, E. Visi-rajczi, L. Albert, Antioxidant properties assessment of the cones of conifers through the combined evaluation of multiple antioxidant assays, Ind. Crop. Prod. 145 (2020) 111935. https://doi.org/10.1016/j.indcrop.2019.111935.

[25] S. Castiglioni, P. Astolfi, C. Conti, E. Monaci, M. Stefano, P. Carloni, Morphological, physicochemical and FTIR spectroscopic properties of bee pollen loads from different botanical origin, Molecules. 24 (2019). https://doi.org/10.3390/molecules24213974.

[26] J. Depciuch, I. Kasprzyk, E. Drzymała, M. Parlinska-Wojtan, Identification of birch pollen species using FTIR spectroscopy, Aerobiologia (Bologna). 34 (2018) 525–538. https://doi.org/10.1007/s10453-018-9528-4.

[27] O. Anjos, A.J.A. Santos, T. Dias, L.M. Estevinho, Application of FTIR-ATR spectroscopy on the bee pollen characterization, J. Apic. Res. 56 (2017) 210–218. https://doi.org/10.1080/00218839.2017.1289657.

[28] R. Lahlali, Y. Jiang, S. Kumar, C. Karunakaran, X. Liu, F. Borondics, E. Hallin, R. Bueckert, ATR-FTIR spectroscopy reveals involvement of lipids and proteins of intact pea pollen grains to heat stress tolerance, Front. Plant Sci. 5 (2014) 1–10. https://doi.org/10.3389/fpls.2014.00747.

[29] C.S. Pappas, P.A. Tarantilis, P.C. Harizanis, M.G. Polissiou, New method for pollen identification by FT-IR spectroscopy, Appl. Spectrosc. 57 (2003) 23–27. https://doi.org/10.1366/000370203321165160.

[30] J.D.I.K.O. Sadik, FTIR analysis of molecular composition changes in hazel pollen from unpolluted and urbanized areas, Aerobiologia (Bologna). 33 (2017) 1–12. https://doi.org/10.1007/s10453-016-9445-3.

[31] M. Kędzierska-Matysek, A. Matwijczuk, M. Florek, J. Barłowska, A. Wolanciuk, A. Matwijczuk, E. Chruściel, R. Walkowiak, D. Karcz, B. Gładyszewska, Application of FTIR spectroscopy for analysis of the quality of honey, BIO Web Conf. 10 (2018) 02008. https://doi.org/10.1051/bioconf/20181002008.

[32] F. Muthreich, B. Zimmermann, H.J.B. Birks, C.M. Vila-Viçosa, A.W.R. Seddon, Chemical variations in Quercus pollen as a tool for taxonomic identification: Implications for long-term ecological and biogeographical research, J. Biogeogr. 47 (2020) 1298–1309. https://doi.org/10.1111/jbi.13817.

[33] C. Engelbrekt, K.H. Sørensen, J. Zhang, A.C. Welinder, P.S. Jensen, J. Ulstrup, Green synthesis of gold nanoparticles with starch – glucose and application in bioelectrochemistry, J. Mater. Chem. 19 (2009) 7839–7847. https://doi.org/10.1039/b911111e.

[34] D. Steinigeweg, M. Schütz, M. Salehi, S. Schlücker, Fast and Cost-Effective Purifi cation of Gold Nanoparticles in the 20 – 250 nm Size Range by Continuous Density Gradient Centrifugation, Small. 7 (2011) 2443–2448. https://doi.org/10.1002/smll.201100663.

[35] X. Su, B. Fu, J. Yuan, Gold nanocluster-coated gold nanorods for simultaneously enhanced photothermal performance and stability, Mater. Lett. 188 (2017) 111–114. https://doi.org/10.1016/j.matlet.2016.11.051.

[36] R. Bhattacharya, C.R. Patra, S. Wang, L. Lu, M.J. Yaszemski, D. Mukhopadhyay, P. Mukherjee, Assembly of gold nanoparticles in a rod-like fashion using proteins as templates, Adv. Funct. Mater. 16 (2006) 395–400. https://doi.org/10.1002/adfm.200500347.

[37] I. Yazgan, A. Gümüş, K. Gökkuş, M.A. Demir, S. Evecen, H.A. Sönmez, R.M. Miller, F. Bakar, A. Oral, S. Popov, M.S. Toprak, On the effect of modified carbohydrates on the size and shape of gold and silver nanostructures, Nanomaterials. 10 (2020) 1–17. https://doi.org/10.3390/nano10071417.

[38] V. Sharma, K. Park, M. Srinivasarao, Shape separation of gold nanorods using centrifugation, Proc. Natl. Acad. Sci. U. S. A. 106 (2009) 4981–4985.

[39] P. Priecel, H. Adekunle, R. Herrera, Z. Zhong, J. Antonio, Anisotropic gold nanoparticles : Preparation and applications in catalysis, Chinese J. Catal. 37 (2016) 1619–1650. https://doi.org/10.1016/S1872-2067(16)62475-0.

[40] N.D. Burrows, A.M. Vartanian, N.S. Abadeer, E.M. Grzincic, L.M. Jacob, W. Lin, J. Li, J.M. Dennison, J.G. Hinman, C.J. Murphy, Anisotropic Nanoparticles and Anisotropic Surface Chemistry, J. Phys. Chem. Lett. 7 (2016) 632–641. https://doi.org/10.1021/acs.jpclett.5b02205.

[41] T. Ming, X. Kou, H. Chen, T. Wang, H.L. Tam, K.W. Cheah, J.Y. Chen, J. Wang, Ordered gold nanostructure assemblies formed by droplet evaporation, Angew. Chemie - Int. Ed. 47 (2008) 9685–9690. https://doi.org/10.1002/anie.200803642.